

Flexibility Management in Economic Dispatch with Dynamic Automatic Generation Control

Lei Fan, *Senior Member, IEEE*; Chaoyue Zhao, *Member, IEEE*; Guangyuan Zhang, *Member, IEEE*; Qihua Huang, *Member, IEEE*

Abstract—As the installation of electronically interconnected renewable energy resources grows rapidly in power systems, system frequency maintenance and control become challenging problems to maintain the system reliability in bulk power systems. As two of the most important frequency control actions in the control centers of independent system operators (ISOs) and utilities, the interaction between Economic Dispatch (ED) and Automatic Generation Control (AGC) attracts more and more attention. In this paper, we propose a robust optimization based framework to measure the system flexibility by considering the interaction between two hierarchical processes (i.e., ED and AGC). We propose a cutting plane algorithm with the reformulation technique to obtain seven different indices of the system. In addition, we study the impacts of several system factors (i.e., the budget of operational cost, ramping capability, and transmission line capacity) and show numerically how these factors can influence the system flexibility.

Index Terms—Economic Dispatch, Automatic Generation Control (AGC), Flexibility Management, Robust Optimization, Cutting Plane Method

I. NOMENCLATURE

A. Sets

- \mathcal{B} Set of buses.
- \mathcal{G} Set of generators.
- \mathcal{G}^b Set of generators at bus b .
- \mathcal{L} Set of transmission lines.

B. Parameters

- CP_n Penalty cost for generator n in dynamic AGC constraints.
- τ Budget for the total operational cost.
- F_l Transmission capacity of transmission line l (MW).
- P_n^{\max} Maximum generation amount (MW) of generator n .
- P_n^{\min} Minimum generation amount (MW) of generator n .
- REG_n^U Maximum regulation up amount of generator n .
- $REG^{\text{Min}U}$ Minimum regulation up requirement of the system.
- REG_n^D Maximum regulation down amount of generator n .
- $REG^{\text{Min}D}$ Minimum regulation down requirement of the system.
- SR_n^{\max} Maximum spinning reserve amount of generator n .

- SR^{\min} Minimum spinning reserve requirement of the system.
- RUR_n Maximum ramping up rate of generator n .
- RDR_n Maximum ramping down rate of generator n .
- $SF_{b,l}$ Shift factors of transmission line l and bus b .
- \bar{d}_b Nominal load amount at bus b .
- $\Delta\bar{d}_t$ Nominal system load change amount at sub time interval t .
- \hat{d}_b The maximum deviation amount from nominal load amount at bus b .
- $\Delta\hat{d}_t$ The maximum load disturbance amount from the nominal value at sub time interval t .
- $\Delta\omega_t^{\min}$ Minimum system frequency change at sub time interval t .
- $\Delta\omega_t^{\max}$ Maximum system frequency change at sub time interval t .

C. Random Parameters

- d_b Random load on bus b (MW).
- Δd_t Random system load disturbance (MW) at sub time interval t .

D. Decision Variables

- oc_n Generation cost function of generator n .
- λ_b^{up} The scale of upper deviation of load at bus b .
- λ_b^{dn} The scale of lower deviation of load at bus b .
- λ_t^{up} The scale of upper deviation of system load within one sub time interval t .
- λ_t^{dn} The scale of lower deviation of system load within one sub time interval t .
- p_n Generation amount of generator n (MW).
- $\Delta f_{n,t}^{GV+}$ Slack variable for dynamic AGC constraints for generator n at sub time interval t .
- $\Delta f_{n,t}^{GV-}$ Slack variable for dynamic AGC constraints for generator n at sub time interval t .
- reg_n^U Regulation up amount of generator n (MW).
- reg_n^D Regulation down amount of generator n (MW).
- sr_n Spinning reserve of generator n (MW).
- $\Delta p_{n,t}^{GV}$ The governor power generation change of generator n at sub time interval t .
- $\Delta p_{n,t}^M$ The prime power generation change of generator n at sub time interval t .
- $\Delta\omega_t$ System frequency change.

II. INTRODUCTION

As the 3D (decarbonization, digitization and decentralization) trend becomes the mainstream in the evolution of energy systems, more and more renewable energy resources are

installed in the bulk power systems. For example, as projected by U.S. Energy Information Administration (EIA) [1], the total share of electricity generation from the renewable energy will be 38% by 2050. In particular, solar energy and wind energy will contribute 17.5% and 12.54% of the total electricity generation by 2050 respectively. Moreover, New York state plans to reach 100% carbon-free by 2050 [2], and California state sets its 100% clean electric power goal by 2045 [3]. The increase of these carbon-free and non-dispatchable energy resources requires the enhancement of the digital management capability of ISOs and utilities.

In order to hedge against the variability and uncertainty of renewable energy generation and therefore achieve a high penetration of renewable energy to the power system, the concept of flexibility has been proposed and investigated, to gauge the capability of the power system in addressing the variability of the net demand (demand net of wind and solar) [4], [5]. From the time scale's perspective, the flexibilities on planning and operations of the power system have been recently investigated. For example, the index of insufficient ramping resource expectation (IRRE) is proposed in [6] to reflect the flexibility of the power system in the generation expansion planning. Operational flexibility and local flexibility for the power system operated by transmission system operators are discussed in [7]. From market design's perspective, ISOs developed different commodity products for the electricity market to capture the flexibility of the resources. For example, CAISO and MISO developed market-based flexible ramping products that can improve the availability of the system's ramping capacity [8]. ERCOT designed a fast frequency response product to maintain sufficient primary frequency control capability under a high penetration of renewable energy [9]. In addition, MISO is investigating short-term reserve products to enhance the system flexibility and ensure reserve deliverability [10]. All these new market designs effectively provide the pricing signal to flexible resources in the energy market system. On the resource level, researchers have investigated flexible generation resources such as combined-cycle power plants [11] and [12], pump-storage plants [13], battery energy storage [14] and [15]. These complex operation models of multi-cycle or multi-stage energy resources in the electricity market not only can strengthen the capability of the grid to respond to the dynamic change of net demand, but also can reduce the operational cost of the electricity grid [16]. In addition, the modeling approaches for aggregations of flexible resources such as virtual power plants and distributed energy resources aggregators have also been studied in [17] and [18].

In this paper, we focus on the real-time flexibility of the power system, motivated by the flexibility metric framework proposed by the researchers from ISO-NE [19]. In [19], the system flexibility is measured in four dimensions (i.e., time, action, uncertainty, and cost). In the time dimension, the short-term flexibility indicates the capability of the system in responding to emergencies or contingencies from minutes to hours. The long-term flexibility indicates the capability of the system in adapting the change of the generation portfolio, system topology, and regulator policy. In the action dimension, different control schemes (e.g., automatic generation control,

economic dispatch, unit commitment, outage management, generation and transmission expansion) can be taken by system operators based on different response time windows to address the variability of the net demand. In the uncertainty dimension, system operators need to manage resources to tackle randomnesses such as equipment failures or forecasting errors of the net demand. Then, the cost restricts the availability of control schemes. With these, the overall system flexibility of the real-time economic dispatch under the uncertainty can be calculated in a systematic way.

In the current electricity market practice, ED, which usually runs every 5 minutes, provides generation resources with the base dispatch point and regulation reserve capacity. However, the traditional ED process does not consider the impact of dynamic AGC, which is executed every 2-6 seconds, with the objective of maintaining the system frequency. This conventional ED-AGC hierarchical model may not be able to provide sufficient system flexibility under a high renewable penetration to track the second-to-second net demand variation [20] and [21]. Therefore, we will study the real-time flexibility management by explicitly considering the interaction between ED and the dynamic AGC. The contributions of our paper can be summarized as follows.

- 1) We propose a robust optimization based framework to measure the system flexibility of the dynamic AGC constrained economic dispatch process. Then, we develop a separation framework to effectively solve the robust feasibility problem.
- 2) We propose seven flexibility indices for a systematic evaluation of the system flexibility, and analyze the system characteristics by using the real-time flexibility management tool to help the system operator understand the impacts of multiple system factors (e.g., budget, ramping capability, and transmission line capability) on the system flexibility.

We organize the remaining part of this paper as follows. Section III describes the mathematical formulation of the system's real-time flexibility based on the AGC constrained economic dispatch. Section IV reports the studies of real-time flexibility in IEEE standard systems. Section V concludes the findings of our paper.

III. MATHEMATICAL FORMULATION OF REAL-TIME FLEXIBILITY

In this section, we deploy a robust optimization based framework to measure the system flexibility of the economic dispatch with the dynamic AGC. In current practice, within every 5-minute interval ED run, the system frequency is adjusted by AGC to its nominal value for every 2-6 seconds. In this paper, we consider the system dynamics within an ED run cycle, i.e., 5 minutes. That is, the overall time horizon is set to be 5 minutes. Within the ED cycle, we consider all the AGC cycles as a set of time interval \mathcal{T} . Both load at each bus and system load disturbance in each time period are assumed to be random and are within an undetermined variation range. That is,

$$d_b \in \mathcal{U}_b(\lambda) = [\bar{d}_b - \lambda_b^{dn} \hat{d}_b, \bar{d}_b + \lambda_b^{up} \hat{d}_b], \quad \forall b \in \mathcal{B}$$

and

$$\Delta d_t \in \mathcal{U}_t(\lambda) = [\Delta \bar{d}_t - \lambda_t^{dn} \Delta \hat{d}_t, \Delta \bar{d}_t + \lambda_t^{up} \Delta \hat{d}_t], \quad \forall t \in \mathcal{T},$$

where \bar{d}_b and \hat{d}_b represent the nominal value and maximum deviation of the load at bus b , and $\Delta \bar{d}_t$ and $\Delta \hat{d}_t$ represent the nominal value and maximum deviation of the system load change at time period t . $\lambda_{\{b,t\}}^{\{up,dn\}} \in [0, 1]$ represent the scales of the deviation for the corresponding variation range. Unlike the traditional robust optimization model that the size of the uncertainty set is predefined, in our model, we will obtain the largest size of each uncertainty set by deciding the scales $\lambda_{\{b,t\}}^{\{up,dn\}}$, to measure the system flexibility that the system can accommodate.

Based on the economic dispatch with dynamic AGC model proposed by [21], we develop a flexibility measurement model as described in III-A.

A. Formulation

$$\max \sum_{b \in \mathcal{B}} (\hat{d}_b \lambda_b^{up} + \hat{d}_b \lambda_b^{dn}) + \sum_{t \in \mathcal{T}} (\Delta \hat{d}_t \lambda_t^{up} + \Delta \hat{d}_t \lambda_t^{dn}) \quad (1a)$$

$$\begin{aligned} s.t. & \sum_{n \in \mathcal{G}} oc_n(p_n) + \sum_{n \in \mathcal{G}} \sum_{t \in \mathcal{T}} CP_n \Delta f_{n,t}^{GV+} \\ & + \sum_{n \in \mathcal{G}} \sum_{t \in \mathcal{T}} CP_n \Delta f_{n,t}^{GV-} \leq \tau \end{aligned} \quad (1b)$$

$$p_n + reg_n^u + sr_n \leq P_n^{\max}, \quad \forall n \in \mathcal{G}, \quad (1c)$$

$$P_n^{\min} \leq p_n - reg_n^d, \quad \forall n \in \mathcal{G}, \quad (1d)$$

$$reg_n^u \leq REG_n^u, \quad \forall n \in \mathcal{G}, \quad (1e)$$

$$reg_n^d \leq REG_n^d, \quad \forall n \in \mathcal{G}, \quad (1f)$$

$$sr_n \leq SR_n^{\max}, \quad \forall n \in \mathcal{G}, \quad (1g)$$

$$\begin{aligned} \Delta p_{n,t+1}^M &= \sum_{i \in \mathcal{G}} (\alpha_{i,n} \Delta p_{i,t}^M + \beta_{i,n} \Delta p_{i,t}^{GV}) + \gamma_n \Delta \omega_t \\ &+ \zeta_n \Delta d_t, \quad \forall n \in \mathcal{G}, \forall \Delta d_t \in \mathcal{U}_t, \forall t \in \mathcal{T}, \end{aligned} \quad (1h)$$

$$\Delta \omega_{t+1} = \sum_{i \in \mathcal{G}} (\kappa_i \Delta p_{i,t}^M + \tau_i \Delta p_{i,t}^{GV}) + \rho \Delta \omega_t + \eta \Delta d_t, \quad (1i)$$

$$\forall \Delta d_t \in \mathcal{U}_t, \forall t \in \mathcal{T},$$

$$\begin{aligned} \Delta p_{n,t+1}^{GV} - \Delta p_{n,t}^{GV} + \Delta f_{n,t+1}^{GV+} - \Delta f_{n,t+1}^{GV-} \\ = K_n \Delta \omega_{t+1}, \quad \forall n \in \mathcal{G}, \forall t \in \mathcal{T} \end{aligned} \quad (1j)$$

$$\Delta p_{n,t+1}^M - \Delta p_{n,t}^M \leq RUR_n, \quad \forall n \in \mathcal{G}, \forall t \in \mathcal{T} \quad (1k)$$

$$\Delta p_{n,t}^M - \Delta p_{n,t+1}^M \leq RDR_n, \quad \forall n \in \mathcal{G}, \forall t \in \mathcal{T} \quad (1l)$$

$$-reg_n^d \leq \Delta p_{n,t}^{GV} \leq reg_n^u, \quad \forall n \in \mathcal{G}, \forall t \in \mathcal{T} \quad (1m)$$

$$\Delta \omega^{\min} \leq \Delta \omega_t \leq \Delta \omega^{\max}, \quad \forall t \in \mathcal{T} \quad (1n)$$

$$\sum_{n \in \mathcal{G}} p_n - \sum_{b \in \mathcal{B}} d_b = 0, \quad \forall d_b \in \mathcal{U}_b, \quad (1o)$$

$$\sum_{n \in \mathcal{G}} sr_n \geq SR^{\min}, \quad (1p)$$

$$\sum_{n \in \mathcal{G}} reg_n^u \geq REG^{\min U}, \quad (1q)$$

$$\sum_{n \in \mathcal{G}} reg_n^d \geq REG^{\min D}, \quad (1r)$$

$$-F_l \leq \sum_{b \in \mathcal{B}} SF_{b,l} (\sum_{n \in \mathcal{G}^b} p_n - d_b) \leq F_l, \quad \forall d_b \in \mathcal{U}_b, \quad (1s)$$

$$\begin{aligned} p_n, reg_n^u, reg_n^d, sr_n, \Delta f_{n,t}^{GV+}, \Delta f_{n,t}^{GV-} \geq 0, \\ \Delta p_{n,t}^{GV}, \Delta p_{n,t}^M, \Delta \omega_t \text{ free}, \\ \lambda_b^{up}, \lambda_b^{dn}, \lambda_t^{up}, \lambda_t^{dn} \in [0, 1], \quad \forall b \in \mathcal{B}, \forall n \in \mathcal{G}, \forall t \in \mathcal{T}, \end{aligned} \quad (1t)$$

where the objective function is to maximize the variation range of the uncertainty. Constraints (1b) represent the budget constraint, which indicates that the total fuel cost and the penalty cost should not exceed a budget τ . Constraints (1c) and (1d) represent the generation limits of traditional thermal units that take account of generation output, regulation and spinning reserves. Constraints (1e), (1f), and (1g) represent the capacities for providing regulation up, regulation down, and spinning reserve services respectively. Constraints (1h) - (1j) represent AGC dynamic system constraints, i.e., the transformation of state vectors $\Delta p_{n,t}^M, \Delta p_{n,t}^{GV}, \Delta \omega_t$ from t to $t+1$ given any demand disturbance Δd_t , where the matrix components $\alpha, \beta, \gamma, \zeta, \kappa, \tau, \rho, \eta$ can be calculated by numerous methods such as zero-order hold method [21]. Constraints (1k) and (1l) restrict ramping up and ramping down limits. Constraints (1m) indicate that the governor generation change should not exceed the regulation service reserved, and constraints (1n) restrict the limit of system frequency change. In addition, the power balance constraints are described in (1o), which should be held for any load realization within the uncertainty set; constraints (1p)-(1r) describe the overall spinning reserve, regulation up, and regulation down requirements respectively, and constraints (1s) represent the transmission capacity constraints.

B. Solution Methodology

First, for notation brevity, we use matrices and vectors to represent constraints and variables, and rewrite the above model in an abstract compact form (denoted as ACF):

$$(ACF) \quad \max a^T \lambda \quad (2a)$$

$$s.t. \quad A_1 x \leq b_1, \quad (2b)$$

$$A_2 x = H_2 d, \quad \forall d_b \in \mathcal{U}_b(\lambda), \forall b \in \mathcal{B}, \quad (2c)$$

$$A_3 x \leq H_3 d, \quad \forall d_b \in \mathcal{U}_b(\lambda), \forall b \in \mathcal{B}, \quad (2d)$$

$$A_4 y = H_4 \Delta d, \quad \Delta d_t \in \mathcal{U}_t(\lambda), \forall t \in \mathcal{T}, \quad (2e)$$

$$A_5 y = b_5, \quad (2f)$$

$$A_6 y \leq b_6, \quad (2g)$$

$$A_7 x + A_8 y \leq b_7, \quad (2h)$$

where $x = (p, reg^u, reg^d, sr)$, $y = (\Delta p^M, \Delta p^{GV}, \Delta \omega, \Delta f^{GV+}, \Delta f^{GV-})$, $d = (d_1, \dots, d_b, \dots)_{b \in \mathcal{B}}$, and $\Delta d = (\Delta d_1, \dots, \Delta d_t, \dots)_{t \in \mathcal{T}}$; objective (2a) represents (1a); constraint (2b) represents (1c) - (1g) and (1p) - (1r); constraint (2c) represents (1o); constraint (2d) represents (1s); constraint (2e) represents (1h) and (1i); constraint (2f) represents (1j); constraint (2g) represents (1k), (1l), and (1n); constraint (2h) represents (1b) and (1m).

We deploy Benders' decomposition framework to solve the problem. Since the problem is to find the largest deviation of the uncertainty set that the system can accommodate, i.e., the largest value of λ without making the constraints (2b)-(2h) infeasible, therefore, only feasibility cuts are needed.

1) *Master Problem and Subproblem*: We first decompose problem ACF into a master problem (denoted as MAP) and a subproblem.

$$(MAP) \quad \max a^T \lambda \quad (3a)$$

$$s.t. \quad g(\lambda) \leq 0 \quad (3b)$$

$$\mathbf{0} \leq \lambda \leq \mathbf{1} \quad (3c)$$

Here, the feasibility cuts are represented in (3b), and $\mathbf{0}$, $\mathbf{1}$ represent vectors with all components 0 and 1 respectively. To generate the feasibility cuts, we first describe the feasibility check problem (denoted as FEA) as follows:

$$(FEA) \quad \max_{d_b \in \mathcal{U}_b, \Delta d_t \in \mathcal{U}_t} \min_{x, y, s} \mathbf{1}^T s \quad (4a)$$

$$s.t. \quad A_1 x - s_1 \leq b_1, \quad (4b)$$

$$A_2 x + s_2^+ - s_2^- = H_2 d, \quad (4c)$$

$$A_3 x - s_3 \leq H_3 d, \quad (4d)$$

$$A_4 y + s_4^+ - s_4^- = H_4 \Delta d, \quad (4e)$$

$$A_5 y + s_5^+ - s_5^- = b_5, \quad (4f)$$

$$A_6 y - s_6 \leq b_6, \quad (4g)$$

$$A_7 x + A_8 y - s_7 \leq b_7. \quad (4h)$$

If λ is feasible, then the optimal value of (FEA) will be 0.

2) *Reformulation of Subproblem*: Now we take the dual of the inner minimization of subproblem (FEA) and combine the dual problem with the outer maximization problem, then we can get the following formulation:

$$(DFEA) \quad \max_{d_b \in \mathcal{U}_b, \Delta d_t \in \mathcal{U}_t, \mu} b_1^T \mu_1 + d^T H_2^T \mu_2 + d^T H_3^T \mu_3 + \Delta d^T H_4^T \mu_4 + b_5^T \mu_5 + b_6^T \mu_6 + b_7^T \mu_7 \quad (5a)$$

$$s.t. \quad A_1^T \mu_1 + A_2^T \mu_2 + A_3^T \mu_3 + A_7^T \mu_7 \leq 0, \quad (5b)$$

$$A_4^T \mu_4 + A_5^T \mu_5 + A_6^T \mu_6 + A_8^T \mu_7 = 0, \quad (5c)$$

$$-\mathbf{1} \leq \mu_1, \mu_3, \mu_6, \mu_7 \leq \mathbf{0}, \quad (5d)$$

$$-\mathbf{1} \leq \mu_2, \mu_4, \mu_5 \leq \mathbf{1}, \quad (5e)$$

where $\mu_1, \mu_2, \mu_3, \mu_4, \mu_5, \mu_6, \mu_7$ are dual variables for constraints (4b) - (4h) respectively.

In the above formulation (DFEA), we have bilinear terms $d^T H_2^T \mu_2$, $d^T H_3^T \mu_3$, and $\Delta d^T H_4^T \mu_4$. We will deal with $d^T H_3^T \mu_3$ first. Let N_i represent the dimension of μ_i and λ^* represent the optimal solution of problem (MAP). Based on the property of d , $\forall b \in \mathcal{B}$, we can rewrite it as $d_b = \bar{d}_b + z_b^+ \lambda_b^{*,up} \hat{d}_b - z_b^- \lambda_b^{*,dn} \hat{d}_b$. Here we introduce two binary variables z_b^+ and z_b^- to indicate the deviation direction. Note that the variables $\lambda_b^{*,up}$ and $\lambda_b^{*,dn}$ have been fixed for DFEA problem. Therefore, we can replace the bilinear term $d^T H_3^T \mu_3$ as follows:

$$\begin{aligned} d^T H_3^T \mu_3 &= \sum_{b \in \mathcal{B}} \sum_{i=1}^{N_3} d_b H_{3,i,b} \mu_{3,i} \\ &= \sum_{b \in \mathcal{B}} \sum_{i=1}^{N_3} (\bar{d}_b H_{3,i,b} \mu_{3,i} + \lambda_b^{*,up} \hat{d}_b H_{3,i,b} z_b^+ \mu_{3,i} \\ &\quad - \lambda_b^{*,dn} \hat{d}_b H_{3,i,b} z_b^- \mu_{3,i}) \end{aligned} \quad (6a)$$

$$z_b^+ + z_b^- = 1, z_b^+, z_b^- \in \{0, 1\} \quad (6b)$$

In (6a), we have two bilinear items $z_b^+ \mu_{3,i}$ and $z_b^- \mu_{3,i}$, which can be further linearized by introducing auxiliary variables $\mu_{3,b,i}^+$ and $\mu_{3,b,i}^-$. By following the approach indicated in [22], we have the following reformulation which is equivalent to (6a):

$$\begin{aligned} d^T H_3^T \mu_3 &= \sum_{b \in \mathcal{B}} \sum_{i=1}^{N_3} (\bar{d}_b H_{3,i,b} \mu_{3,i} + \\ &\quad \lambda_b^{*,up} \hat{d}_b H_{3,i,b} \mu_{3,b,i}^+ - \lambda_b^{*,dn} \hat{d}_b H_{3,i,b} \mu_{3,b,i}^-) \end{aligned} \quad (7a)$$

$$-z_b^+ \leq \mu_{3,b,i}^+, \mu_{3,i} \leq \mu_{3,b,i}^+ \leq 1 - z_b^+ + \mu_{3,i}, \quad (7b)$$

$$-z_b^- \leq \mu_{3,b,i}^-, \mu_{3,i} \leq \mu_{3,b,i}^- \leq 1 - z_b^- + \mu_{3,i}, \quad (7c)$$

$$z_b^+ + z_b^- = 1, z_b^+, z_b^- \in \{0, 1\}, \quad (7d)$$

$$-1 \leq \mu_{3,b,i}^+, \mu_{3,b,i}^- \leq 0, \forall b \in \mathcal{B}, \forall i = 1, \dots, N_3. \quad (7e)$$

For $d^T H_2^T \mu_2$ and $\Delta d^T H_4^T \mu_4$, we can use a similar approach. We will use $d^T H_2^T \mu_2$ as an example and the other follows the same approach. Since $\mu_2 \in [-1, 1]$, we can replace it with $\mu_2^n - \mu_2^p$ and $-\mathbf{1} \leq \mu_2^n \leq \mathbf{0}$ and $-\mathbf{1} \leq \mu_2^p \leq \mathbf{0}$. Then $d^T H_2^T \mu_2 = d^T H_2^T \mu_2^n - d^T H_2^T \mu_2^p$. For $d^T H_2^T \mu_2^n$ and $d^T H_2^T \mu_2^p$, we will follow the same procedure of (7a)-(7e) to linearize them. Therefore, we can reformulate the (DFEA) problem as follows:

$$\begin{aligned} (RDFEA) \quad \max_{d_b, \Delta d_t, \mu} &b_1^T \mu_1 + \sum_{b \in \mathcal{B}} \sum_{i=1}^{N_2} \{\bar{d}_b H_{2,i,b} (\mu_{2,i}^n - \mu_{2,i}^p) + \\ &\lambda_b^{*,up} \hat{d}_b H_{2,i,b} (\mu_{2,b,i}^{n,+} - \mu_{2,b,i}^{p,+}) - \lambda_b^{*,dn} \hat{d}_b H_{2,i,b} (\mu_{2,b,i}^{n,-} - \mu_{2,b,i}^{p,-})\} \\ &+ \sum_{b \in \mathcal{B}} \sum_{i=1}^{N_3} (\bar{d}_b H_{3,i,b} \mu_{3,i} + \lambda_b^{*,up} \hat{d}_b H_{3,i,b} \mu_{3,b,i}^+ \\ &- \lambda_b^{*,dn} \hat{d}_b H_{3,i,b} \mu_{3,b,i}^-) + \sum_{t \in \mathcal{T}} \sum_{i=1}^{N_4} \{\Delta \bar{d}_t H_{4,i,t} (\mu_{4,i}^n - \mu_{4,i}^p) \\ &+ \lambda_t^{*,up} \Delta \hat{d}_t H_{4,i,t} (\mu_{4,t,i}^{n,+} - \mu_{4,t,i}^{p,+}) \\ &- \lambda_t^{*,dn} \Delta \hat{d}_t H_{4,i,t} (\mu_{4,t,i}^{n,-} - \mu_{4,t,i}^{p,-})\} + b_5 \mu_5 + b_6 \mu_6 + b_7 \mu_7 \end{aligned} \quad (8a)$$

$$s.t. \quad A_1^T \mu_1 + A_2^T \mu_2 + A_3^T \mu_3 + A_7^T \mu_7 \leq 0, \quad (8a)$$

$$A_4^T \mu_4 + A_5^T \mu_5 + A_6^T \mu_6 + A_8^T \mu_7 = 0, \quad (8b)$$

$$-z_b^+ \leq \mu_{2,b,i}^n, \mu_{2,i}^n \leq \mu_{2,b,i}^n \leq 1 - z_b^+ + \mu_{2,i}^n, \quad (8c)$$

$$-z_b^- \leq \mu_{2,b,i}^p, \mu_{2,i}^p \leq \mu_{2,b,i}^p \leq 1 - z_b^- + \mu_{2,i}^p, \quad (8d)$$

$$-z_b^+ \leq \mu_{2,b,i}^{p,+}, \mu_{2,i}^p \leq \mu_{2,b,i}^{p,+} \leq 1 - z_b^+ + \mu_{2,i}^p, \quad (8e)$$

$$-z_b^- \leq \mu_{2,b,i}^{p,-}, \mu_{2,i}^p \leq \mu_{2,b,i}^{p,-} \leq 1 - z_b^- + \mu_{2,i}^p, \quad (8f)$$

$$\forall b \in \mathcal{B}, \forall i = 1, \dots, N_2,$$

$$-z_b^+ \leq \mu_{3,b,i}^+, \mu_{3,i} \leq \mu_{3,b,i}^+ \leq 1 - z_b^+ + \mu_{3,i}, \quad (8g)$$

$$-z_b^- \leq \mu_{3,b,i}^-, \mu_{3,i} \leq \mu_{3,b,i}^- \leq 1 - z_b^- + \mu_{3,i}, \quad (8h)$$

$$\forall b \in \mathcal{B}, \forall i = 1, \dots, N_3,$$

$$-z_t^+ \leq \mu_{4,t,i}^n, \mu_{4,i}^n \leq \mu_{4,t,i}^n \leq 1 - z_t^+ + \mu_{4,i}^n, \quad (8i)$$

$$-z_t^- \leq \mu_{4,t,i}^p, \mu_{4,i}^p \leq \mu_{4,t,i}^p \leq 1 - z_t^- + \mu_{4,i}^p, \quad (8j)$$

$$-z_t^+ \leq \mu_{4,t,i}^{p,+}, \mu_{4,i}^p \leq \mu_{4,t,i}^{p,+} \leq 1 - z_t^+ + \mu_{4,i}^p, \quad (8k)$$

$$-z_t^- \leq \mu_{4,t,i}^{p,-}, \mu_{4,i}^p \leq \mu_{4,t,i}^{p,-} \leq 1 - z_t^- + \mu_{4,i}^p, \quad (8l)$$

$$\forall t \in \mathcal{T}, \forall i = 1, \dots, N_4,$$

$$z_b^+ + z_b^- = 1, z_t^+ + z_t^- = 1, \forall b \in \mathcal{B}, \forall t \in \mathcal{T}, \quad (8m)$$

$$-\mathbf{1} \leq \mu_2^{n,+}, \mu_2^{n,-}, \mu_2^{p,+}, \mu_2^{p,-} \leq \mathbf{0}, \quad (8n)$$

$$-\mathbf{1} \leq \mu_3^+, \mu_3^- \leq \mathbf{0},$$

$$-\mathbf{1} \leq \mu_4^{n,+}, \mu_4^{n,-}, \mu_4^{p,+}, \mu_4^{p,-} \leq \mathbf{0}, \quad (8o)$$

$$-\mathbf{1} \leq \mu_1, \mu_3, \mu_6, \mu_7 \leq \mathbf{0}, \quad (8p)$$

$$-\mathbf{1} \leq \mu_2, \mu_4, \mu_5 \leq \mathbf{1}. \quad (8q)$$

If the objective value η^* of subproblem (RDFEA) is greater than 0, we can obtain the following feasibility cut:

$$\begin{aligned} \eta(\lambda) = & \sum_{b \in \mathcal{B}} \left(\sum_{i=1}^{N_2} \hat{d}_b H_{2,i,b} (\mu_{2,b,i}^{n+,*} - \mu_{2,b,i}^{p+,*}) + \sum_{i=1}^{N_3} \hat{d}_b H_{3,i,b} \mu_{3,b,i}^{+,*} \right) \lambda_b^{up} \\ & - \sum_{b \in \mathcal{B}} \left(\sum_{i=1}^{N_2} \hat{d}_b H_{2,i,b} (\mu_{2,b,i}^{n-,*} - \mu_{2,b,i}^{p-,*}) + \sum_{i=1}^{N_3} \hat{d}_b H_{3,i,b} \mu_{3,b,i}^{-,*} \right) \lambda_b^{dn} \\ & + \sum_{t \in \mathcal{T}} \sum_{i=1}^{N_4} \Delta \hat{d}_t H_{4,i,t} (\mu_{4,t,i}^{n+,*} - \mu_{4,t,i}^{p+,*}) \lambda_t^{up} \\ & - \sum_{t \in \mathcal{T}} \sum_{i=1}^{N_4} \Delta \hat{d}_t H_{4,i,t} (\mu_{4,t,i}^{n-,*} - \mu_{4,t,i}^{p-,*}) \lambda_t^{dn} \\ & + b_1^T \mu_1^* + \sum_{b \in \mathcal{B}} \sum_{i=1}^{N_2} \bar{d}_b H_{2,i,b} (\mu_{2,i}^{n*} - \mu_{2,i}^{p*}) \\ & + \sum_{b \in \mathcal{B}} \sum_{i=1}^{N_3} \bar{d}_b H_{3,i,b} \mu_{3,i}^* + \sum_{t \in \mathcal{T}} \sum_{i=1}^{N_4} \Delta \bar{d}_t H_{4,i,t} (\mu_{4,i}^{n*} - \mu_{4,i}^{p*}) \\ & + b_5 \mu_5^* + b_6 \mu_6^* + b_7 \mu_7^* \leq 0 \end{aligned} \quad (9)$$

3) *Algorithm Framework*: We summarize our Benders' decomposition based framework as follows:

- 1) Solve the master problem (MAP) and obtain the optimal solution λ^* .
- 2) Test the feasibility of the subproblem by solving dual reformulated DFEA problem with λ^* .
- 3) If the optimal value η^* of DFEA > 0 , then update the master problem by adding feasibility cut (9) and go to Step 2. Otherwise, terminate and return the optimal solution and objective value of master problem.

IV. CASE STUDY

In this section, we test the performance of the proposed real-time flexibility management model with the IEEE 118-bus system (online [23]). These cases are tested by using Julia [24] and CPLEX 12.8 [25] on Intel Xeon Silver 4216 CPU and 128 G memory.

To get the insights on how the system operators can improve their system flexibility by using limited resources, we investigate on which factors will have impacts on the system flexibility. More specifically, we study key factors including the budget of operational cost, ramping capability, and transmission line capacity. In order to obtain more information on the system's capability in handling uncertainty, we analyze seven different system flexibility indicators: total flexibility (TF), economic dispatch flexibility (EDF), AGC flexibility (AGCF),

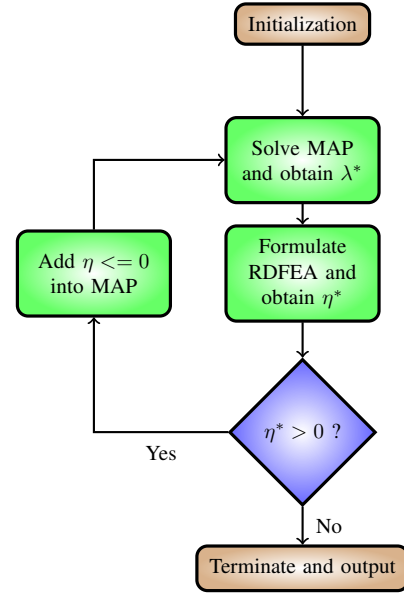


Fig. 1. Flowchart of Decomposition Algorithm

economic dispatch upward flexibility (EDUPF), economic dispatch downward flexibility (EDDNF), AGC upward flexibility (AGCUPF), and AGC downward flexibility (AGCDNF) based on the simulation results. The definitions of these flexibility indicators are shown in (10a) - (10g).

$$\text{TF} = \sum_b (\hat{d}_b \lambda_b^{up} + \hat{d}_b \lambda_b^{dn}) + \sum_{t \in \mathcal{T}} (\Delta \hat{d}_t \lambda_t^{up} + \Delta \hat{d}_t \lambda_t^{dn}) \quad (10a)$$

$$\text{EDF} = \sum_b (\hat{d}_b \lambda_b^{up} + \hat{d}_b \lambda_b^{dn}) \quad (10b)$$

$$\text{AGCF} = \sum_{t \in \mathcal{T}} (\Delta \hat{d}_t \lambda_t^{up} + \Delta \hat{d}_t \lambda_t^{dn}) \quad (10c)$$

$$\text{EDUPF} = \sum_b (\hat{d}_b \lambda_b^{up}) \quad (10d)$$

$$\text{EDDNF} = \sum_b (\hat{d}_b \lambda_b^{dn}) \quad (10e)$$

$$\text{AGCUPF} = \sum_{t \in \mathcal{T}} (\Delta \hat{d}_t \lambda_t^{up}) \quad (10f)$$

$$\text{AGCDNF} = \sum_{t \in \mathcal{T}} (\Delta \hat{d}_t \lambda_t^{dn}) \quad (10g)$$

The TF can gauge both static and dynamic system capability to handle the uncertainty caused by forecasting errors of load and renewable resources. The EDF reflects the static capability of the system. The AGCF indicates the capability of the system to respond to the disturbance in real time. The EDUPF and EDDNF can explain up and down static flexibility of the system. The AGCUPF and AGCDNF can describe the up and down dynamic flexibility of the system, respectively.

In the nominal case, there are 30 units online and the system load is around 86.3% of the total capacity of online units. We assume the uncertain range of the net load at each bus is $[-15\%, 15\%]$ and the system load disturbance is within the range $[-1\%, 1\%]$.

A. Impact of Operational Cost

In this subsection, we first investigate the impact of the operational cost budget by increasing it gradually (denoted from B0 to B22 in Column 1, Table I). We set the budget of the base case (denoted as B0) as the optimal operational cost of the economic dispatch under the nominal foretasted net load without the dynamic AGC. Then we incrementally scale up the budget by using the scale factor (SF) as shown in Column 2 in Table I. For example, the budget of B22 is four times of the budget of B0. All other system parameters are the same in these 23 cases. We report the simulation results of the proposed flexibility indicators under different budgets in Table I.

TABLE I
SYSTEM FLEXIBILITY UNDER DIFFERENT BUDGETS

Budget	SF	TF	EDF	AGCF	EDUPF	EDDNF	AGCUPF	AGCDNF
B0	1.00	115.298	115.298	0.000	47.626	67.672	0.000	0.000
B1	1.01	120.678	120.678	0.000	53.006	67.672	0.000	0.000
B2	1.02	125.532	125.532	0.000	57.861	67.672	0.000	0.000
B3	1.03	129.411	129.411	0.000	61.739	67.672	0.000	0.000
B4	1.04	129.520	129.476	0.044	61.804	67.672	0.026	0.018
B5	1.05	129.550	129.476	0.074	61.804	67.672	0.048	0.026
B6	1.06	129.579	129.476	0.103	61.804	67.672	0.078	0.026
B7	1.07	129.609	129.476	0.133	61.804	67.672	0.059	0.074
B8	1.08	129.638	129.476	0.162	61.804	67.672	0.086	0.076
B9	1.09	129.668	129.476	0.192	61.804	67.672	0.093	0.099
B10	1.10	129.697	129.476	0.221	61.804	67.672	0.109	0.112
B11	1.20	129.993	129.476	0.517	61.804	67.672	0.290	0.227
B12	1.30	130.288	129.476	0.812	61.804	67.672	0.400	0.412
B13	1.40	130.583	129.476	1.107	61.804	67.672	0.578	0.529
B14	1.50	130.878	129.476	1.402	61.804	67.672	0.730	0.672
B15	1.60	131.174	129.476	1.698	61.804	67.672	0.682	1.015
B16	1.70	131.469	129.476	1.993	61.804	67.672	0.844	1.149
B17	1.80	131.764	129.476	2.288	61.804	67.672	1.133	1.156
B18	1.90	131.976	129.476	2.500	61.804	67.672	1.250	1.250
B19	2.00	131.976	129.476	2.500	61.804	67.672	1.250	1.250
B20	2.50	131.976	129.476	2.500	61.804	67.672	1.250	1.250
B21	3.00	131.976	129.476	2.500	61.804	67.672	1.250	1.250
B22	4.00	131.976	129.476	2.500	61.804	67.672	1.250	1.250

From Columns 1-5 in Table I, we can observe that three flexibility indicators (i.e., TF, EDF, and AGCF) are non-decreasing as the budget increases. On one hand, for EDF, when the budget is small and gradually increases by 1% from B0 to B3, the EDF increases by around 4% for each level of the budget. Once the scale factor (SF) reaches 1.04, EDF remains as a constant number. On the other hand, when the budget remains small, i.e., B0-B3, AGCF remains 0. But when the budget becomes larger, AGCF increases and becomes a constant when a relatively large budget (i.e., B18 and above) is available. That is because that when the budget is small, EDF will be allocated to all operational cost budget as it has more weight than AGCF in the objective function. But when the system has more budget for operational cost, which is sufficient for the operational cost of the economic dispatch, it will start to allocate budget to the dynamic AGC part. Therefore, with more budget available, AGCF will incur more operational costs. But when the total budget is sufficient for both ED and AGC costs, both EDF and AGCF will not increase. In addition, the increment of AGCF will result in the increment of TF. We show the trends of indicators TF, EDF, and AGCF in Fig. 2.

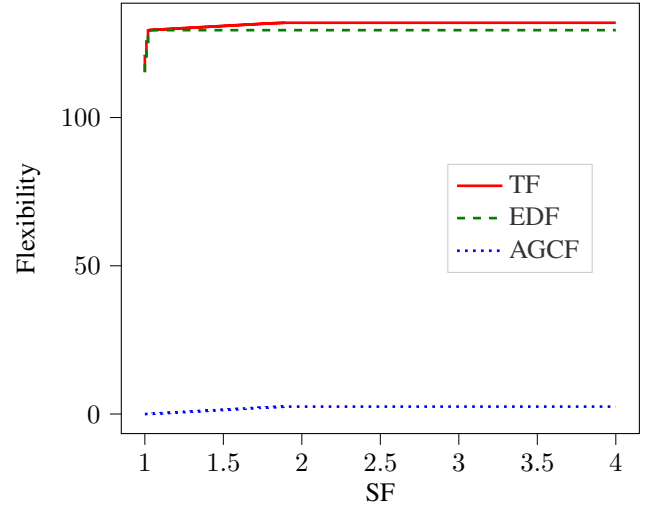


Fig. 2. Trends of TF, EDF, and AGCF

We further analyze the trend of EDF by looking into its two components: EDUPF and EDDNF, and we show the trends of these three factors in Fig. 3. From the figure, we can observe that EDDNF does not change as the budget changes but EDUPF increases and becomes stable when a higher budget is available. That is because the operational cost only includes the fuel cost of thermal units, which means that it can reflect the cost caused by increasing the thermal generators' output. In other words, the economic dispatch upward flexibility can be restricted by the system budget when the system experiences a high load and a low renewable energy output. Therefore, the budget of the operational cost has a significant impact on EDUPF, especially when the budget is close to the cost of the economic dispatch only without dynamic AGC. On the contrary, since there is no cost when generators reduce their output, the budget has little impact on the economic dispatch downward flexibility.

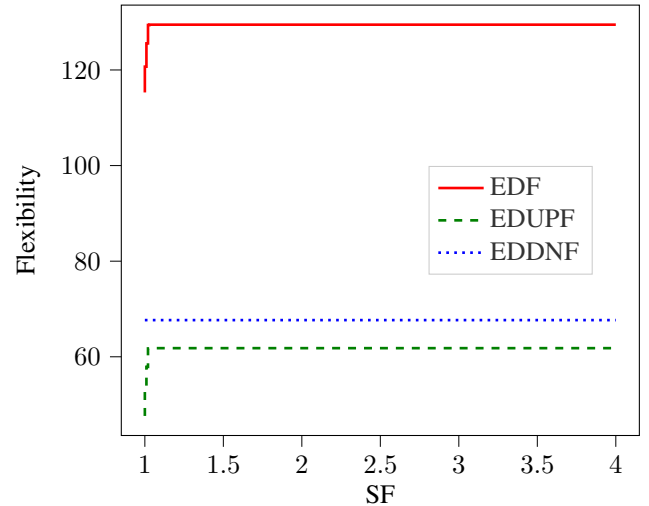


Fig. 3. Trends of EDF, EDUPF, and EDDNF

In addition, we show the trends of AGCF, AGCUPF, and

AGCDNF in Fig. 4. We can observe that the AGCF is monotonic non-decreasing as the budget increases. Similarly, AGCUPF and AGCDNF both increase (not monotonic) as the budget increases. Once the scale factor of the budget reaches B18, all flexibility indicators remain as constants.

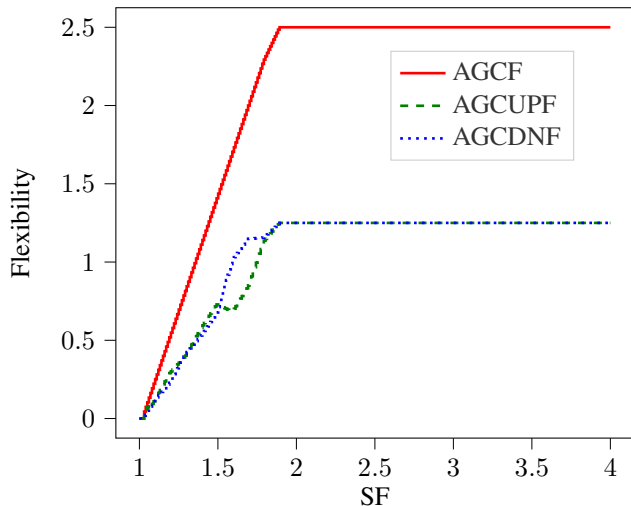


Fig. 4. Trends of AGCF, AGCUPF, and AGCDNF

B. Impacts of Ramping Capability

In this subsection, we report simulation results by increasing the ramping capability of generators under three different budget settings (i.e., B0, B14, and B19). Then, we test different ramping capability settings of all generators in the system to check how flexibility indicators change with ramping capability under a fixed budget. We report flexibility indicators (i.e., TF, EDF, and AGCF) in Table II and show the TF curves in Fig. 5.

Fig. 5 shows that the increasing ramping capability can improve both TF and EDF of the system, but it has a limited effect on enhancing AGCF. Under both budgets (B0 and B14), AGCF increases as the SF increases, while under budget B19, the AGCF remains the same with the change of ramping capability. Therefore, we can observe that the ramping capacity will influence the economic dispatch significantly but influence the dynamic AGC minimally.

C. Impacts of Transmission Line Capacity

In this subsection, we study the impact of transmission line capacity on the system flexibility. Similar to the setup of ramping capability experiments, we study the system flexibility under three different budgets (i.e., B0, B14, and B19). Then we test different scenarios of all the transmission line capacity in Table III by changing the scale factor.

We can observe that under the budget B0 and B19, AGCF remains unchanged, and under budget B14, it changes slightly. This also indicates that improving the transmission capacity has a marginal impact on the AGCF. On the contrary, Fig. 6 demonstrates that a larger transmission line capacity can improve TF for a fixed budget until TF reaches its maximum value.

TABLE II
SYSTEM FLEXIBILITY UNDER DIFFERENT RAMPING CAPABILITIES

SF	B0			B14			B19		
	TF	EDF	AGCF	TF	EDF	AGCF	TF	EDF	AGCF
1	115.298	115.298	0.000	130.878	129.476	1.402	131.976	129.476	2.500
1.01	115.431	115.431	0.000	130.904	129.501	1.403	132.001	129.501	2.500
1.02	115.564	115.563	0.000	130.930	129.526	1.404	132.026	129.526	2.500
1.03	115.697	115.696	0.000	130.956	129.551	1.405	132.051	129.551	2.500
1.04	115.830	115.829	0.001	130.982	129.576	1.406	132.076	129.576	2.500
1.05	115.963	115.962	0.001	131.007	129.601	1.406	132.101	129.601	2.500
1.06	116.096	116.095	0.001	131.033	129.626	1.407	132.126	129.626	2.500
1.07	116.229	116.227	0.001	131.059	129.651	1.408	132.151	129.651	2.500
1.08	116.362	116.360	0.001	131.085	129.676	1.409	132.176	129.676	2.500
1.09	116.494	116.493	0.001	131.111	129.701	1.410	132.201	129.701	2.500
1.1	116.623	116.622	0.002	131.136	129.726	1.410	132.226	129.726	2.500
1.2	117.906	117.902	0.003	131.394	129.976	1.418	132.476	129.976	2.500
1.3	119.152	119.147	0.005	131.652	130.226	1.426	132.726	130.226	2.500
1.4	120.367	120.361	0.006	131.909	130.476	1.433	132.976	130.476	2.500
1.5	121.573	121.566	0.006	132.166	130.726	1.440	133.226	130.726	2.500
1.6	122.746	122.739	0.007	132.423	130.976	1.447	133.476	130.976	2.500
1.7	123.864	123.857	0.007	132.680	131.226	1.454	133.726	131.226	2.500
1.8	124.962	124.955	0.008	132.936	131.476	1.460	133.976	131.476	2.500
1.9	126.054	126.046	0.008	133.193	131.726	1.467	134.226	131.726	2.500
2	127.121	127.113	0.008	133.449	131.976	1.473	134.476	131.976	2.500
2.5	131.161	131.151	0.011	133.775	132.259	1.515	134.760	132.259	2.500
3	132.315	132.259	0.056	133.811	132.259	1.552	134.760	132.259	2.500
4	132.393	132.259	0.133	133.874	132.259	1.615	134.760	132.259	2.500

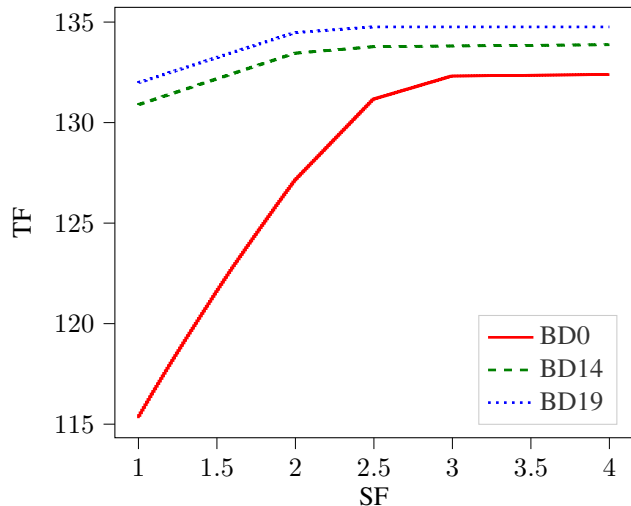


Fig. 5. Trends of TF under Different Ramping Capabilities

V. CONCLUSIONS

In this paper, we proposed a real-time flexibility management framework to model economic dispatch with dynamic AGC constraints. The proposed framework can be solved by conducting reformulation and decomposition. We further proposed seven system flexibility indices (i.e., TF, EDF, AGCF, EDUPF, EDDNF, AGCUPF, AGCDNF) to reflect the system flexibility and studied how the system factors such that the operational cost budget, ramping capacity and transmission line capacity can impact the system flexibility. We found that the budget of the operational cost can significantly contribute to all indicators expect EDDNF, and the improvement of ramping capacity can significantly enhance the EDF and the AGCF. In addition, we discover that the transmission capacity only contributes to EDF. As the future work, we will study the power system flexibility with considering the inertia of

TABLE III
SYSTEM FLEXIBILITY UNDER DIFFERENT TRANSMISSION LINE
CAPABILITIES

SF	B0			B14			B19		
	TF	EDF	AGCF	TF	EDF	AGCF	TF	EDF	AGCF
1	115.298	115.298	0.000	130.878	129.476	1.402	131.976	129.476	2.500
1.01	115.560	115.560	0.000	131.076	129.673	1.402	132.173	129.673	2.500
1.02	115.823	115.823	0.000	131.273	129.870	1.403	132.371	129.870	2.500
1.03	116.054	116.054	0.000	131.470	130.068	1.403	132.568	130.068	2.500
1.04	116.251	116.251	0.000	131.667	130.265	1.403	132.765	130.265	2.500
1.05	116.448	116.448	0.000	131.865	130.462	1.403	132.962	130.462	2.500
1.06	116.645	116.645	0.000	132.062	130.659	1.403	133.159	130.659	2.500
1.07	116.842	116.842	0.000	132.259	130.856	1.403	133.356	130.856	2.500
1.08	117.038	117.038	0.000	132.456	131.053	1.403	133.554	131.053	2.500
1.09	117.217	117.217	0.000	132.653	131.251	1.403	133.751	131.251	2.500
1.1	117.392	117.392	0.000	132.851	131.448	1.403	133.948	131.448	2.500
1.2	118.913	118.913	0.000	133.672	132.259	1.413	134.760	132.259	2.500
1.3	119.008	119.008	0.000	133.683	132.259	1.424	134.760	132.259	2.500
1.4	119.008	119.008	0.000	133.687	132.259	1.428	134.760	132.259	2.500
1.5	119.008	119.008	0.000	133.687	132.259	1.428	134.760	132.259	2.500
1.6	119.008	119.008	0.000	133.687	132.259	1.428	134.760	132.259	2.500
1.7	119.008	119.008	0.000	133.687	132.259	1.428	134.760	132.259	2.500
1.8	119.008	119.008	0.000	133.687	132.259	1.428	134.760	132.259	2.500
1.9	119.008	119.008	0.000	133.687	132.259	1.428	134.760	132.259	2.500
2	119.008	119.008	0.000	133.687	132.259	1.428	134.760	132.259	2.500
2.5	119.008	119.008	0.000	133.687	132.259	1.428	134.760	132.259	2.500
3	119.008	119.008	0.000	133.687	132.259	1.428	134.760	132.259	2.500
4	119.008	119.008	0.000	133.687	132.259	1.428	134.760	132.259	2.500

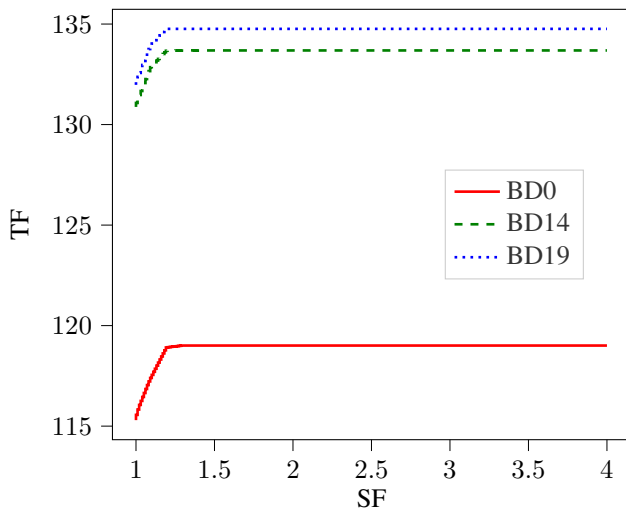


Fig. 6. Trends of TF under Different Transmission Line Capabilities

the resources in the system.

REFERENCES

- [1] "Annual Energy Outlook 2020." [Online]. Available: <https://www.eia.gov/outlooks/aeo/>.
- [2] S. F. Tierney and P. J. Hibbard, "The role and economic impacts of a carbon price in nyiso's wholesale electricity markets," 2019. [Online]. Available: <https://www.nyiso.com/>
- [3] CAISO, "SB 100 joint agency report: Charting a path to a 100% clean energy future," 2019. [Online]. Available: <https://www.energy.ca.gov/event/workshop/2019-09/>
- [4] B. F. Hobbs, J. C. Honious, and J. Bluestein, "What's flexibility worth? the enticing case of natural gas cofiring," *The Electricity Journal*, vol. 5, no. 2, pp. 37–47, 1992.
- [5] E. Ela, M. Milligan, A. Bloom, A. Botterud, A. Townsend, and T. Levin, "Evolution of wholesale electricity market design with increasing levels of renewable generation," National Renewable Energy Lab.(NREL), Golden, CO (United States), Tech. Rep., 2014.

- [6] E. Lannoye, D. Flynn, and M. O'Malley, "Evaluation of power system flexibility," *IEEE Transactions on Power Systems*, vol. 27, no. 2, pp. 922–931, 2012.
- [7] M. A. Bucher, S. Delikaraoglou, K. Heussen, P. Pinson, and G. Andersson, "On quantification of flexibility in power systems," in *2015 IEEE Eindhoven PowerTech*. IEEE, 2015, pp. 1–6.
- [8] Q. Wang and B.-M. Hodge, "Enhancing power system operational flexibility with flexible ramping products: A review," *IEEE Transactions on Industrial Informatics*, vol. 13, no. 4, pp. 1652–1664, 2016.
- [9] C. Liu and P. Du, "Participation of load resources in day-ahead market to provide primary-frequency response reserve," *IEEE Transactions on Power Systems*, vol. 33, no. 5, pp. 5041–5051, 2018.
- [10] F. Wang, A. Korad, and Y. Chen, "Reserve deliverability with application to short-term reserve product," 2019. [Online]. Available: <https://www.ferc.gov/>
- [11] L. Fan and Y. Guan, "An edge-based formulation for combined-cycle units," *IEEE Transactions on Power Systems*, vol. 31, no. 3, pp. 1809–1819, 2015.
- [12] C. Dai, Y. Chen, F. Wang, J. Wan, and L. Wu, "A configuration-component-based hybrid model for combined-cycle units in miso day-ahead market," *IEEE Transactions on Power Systems*, vol. 34, no. 2, pp. 883–896, 2018.
- [13] J. Garcia-Gonzalez, R. M. R. de la Muela, L. M. Santos, and A. M. Gonzalez, "Stochastic joint optimization of wind generation and pumped-storage units in an electricity market," *IEEE Transactions on Power Systems*, vol. 23, no. 2, pp. 460–468, 2008.
- [14] T. Ding, J. Bai, P. Du, B. Qin, F. Li, J. Ma, and Z. Dong, "Rectangle packing problem for battery charging dispatch considering uninterrupted discrete charging rate," *IEEE Transactions on Power Systems*, vol. 34, no. 3, pp. 2472–2475, 2019.
- [15] B. Xu, J. Zhao, T. Zheng, E. Litvinov, and D. S. Kirschen, "Factoring the cycle aging cost of batteries participating in electricity markets," *IEEE Transactions on Power Systems*, vol. 33, no. 2, pp. 2248–2259, 2017.
- [16] Y. Guan, L. Fan, and Y. Yu, "Unified formulations for combined-cycle units," *IEEE Transactions on Power Systems*, vol. 33, no. 6, pp. 7288–7291, 2018.
- [17] S. Babaei, C. Zhao, and L. Fan, "A data-driven model of virtual power plants in day-ahead unit commitment," *IEEE Transactions on Power Systems*, vol. 34, no. 6, pp. 5125–5135, 2019.
- [18] X. Chen, E. Dall'Anese, C. Zhao, and N. Li, "Aggregate power flexibility in unbalanced distribution systems," *IEEE Transactions on Smart Grid*, vol. 11, no. 1, pp. 258–269, 2019.
- [19] J. Zhao, T. Zheng, and E. Litvinov, "A unified framework for defining and measuring flexibility in power system," *IEEE Transactions on Power Systems*, vol. 31, no. 1, pp. 339–347, 2015.
- [20] W. Li and Y. Chen, "MISO AGC enhancement proposal to better utilize fast ramping resources," in *2015 IEEE Power & Energy Society General Meeting*. IEEE, 2015, pp. 1–5.
- [21] G. Zhang, J. McCalley, and Q. Wang, "An agc dynamics-constrained economic dispatch model," *IEEE Transactions on Power Systems*, vol. 34, no. 5, pp. 3931–3940, Sep. 2019.
- [22] L. Fan, J. Wang, R. Jiang, and Y. Guan, "Min-max regret bidding strategy for thermal generator considering price uncertainty," *IEEE Transactions on Power Systems*, vol. 29, no. 5, pp. 2169–2179, Sep. 2014.
- [23] "IEEE 118-bus system." [Online]. Available: <http://motor.ece.iit.edu/data/>
- [24] M. Lubin and I. Dunning, "Computing in operations research using julia," *INFORMS Journal on Computing*, vol. 27, no. 2, pp. 238–248, 2015.
- [25] IBM, "IBM CPLEX optimizer." [Online]. Available: <https://www.ibm.com/analytics/cplex-optimizer>